Published in IET Microwaves, Antennas & Propagation
Received on 9th April 2011
Revised on 24th July 2011
doi: 10.1049/iet-map.2011.0171

ISSN 1751-8725

Reactance domains unitary MUSIC algorithms based on real-valued orthogonal decomposition for electronically steerable parasitic array radiator antennas

S. Akkar A. Gharsallah

Unit of Research in High Frequency Electronic Circuits and Systems, Faculty of Sciences of Tunis El Manar University, Tunisia 2092
E-mail: salemakkar@yahoo.fr

Abstract: This study proposes three algorithms, requiring only real-valued operations, to estimate the directions of arrival (DoAs) of correlated sources impinging onto electronically steerable parasitic array radiator (ESPAR) antennas. The constraints on the proposed algorithms are the same as those imposed onto the reactance domains-MUSIC (RD-MUSIC) algorithm allowing superior high-resolution localisation capabilities even for correlated sources scenarios with reduced computational cost as well as a low processing time compared with existing schemes. The first of the three proposed algorithms is a real-valued formulation of the standard MUSIC algorithm for ESPAR antennas that reduces significantly the computational complexity in the eigen-analysis stage. However, the other two algorithms are based on real-valued orthogonal decompositions (RVOD) techniques to estimate the noise subspace of the covariance matrices. We demonstrate that both the RVOD techniques can efficiently replace the requirement of singular value decomposition or eigenvalue decomposition which reduces further the computational complexity and makes the DoAs estimation faster. The Cramer Rao bound on the variance of DoAs estimated by the three proposed algorithms is analysed. The asymptotic performance of the developed methods is studied and compared with conventional antenna arrays. The simulation results confirm that the developed methods achieve superior precision and accuracy in DoAs estimation compared to RD-MUSIC even for correlated signals and prove the validity of our approach.

1 Introduction

Reducing the calculation complexity and the processing time of direction-of-arrivals (DoAs) estimators without sacrificing performance is a challenging topic that has attracted considerable attention. In recent years, researchers have developed various high-resolution DoAs estimators based on eigen-decomposition of the array covariance matrix, such as multiple signal classification (MUSIC), estimation of signal parameters via rotational invariance techniques (ESPRITs) and propagator [1–4] along with some of their variants such as extended-MUSIC [3, 4]. Particularly, over the last decade, a great deal of effort [5–10] has been focused on taking advantages of eletronically steerable parasitic array radiator (ESPAR) antennas to improve the performance of localisation systems. Unlike conventional antennas arrays, ESPAR antennas are free from the negative influences of the mutual coupling because they are fundamentally based on this phenomenon. Therefore there is no need to use any antenna arrays calibration process. In addition, ESPAR antennas offer many other advantages over conventional arrays such as a low-power consumption (only the active element is fed), low cost (only one receiver chain placed in the output of active element), small size and ease of fabrication. Specifically, ESPAR antennas first developed for applications in wireless *ad-hoc* networks and they are consciously used to reduce energy consumption. Furthermore, the low-power consumption, in comparison with conventional arrays, makes ESPAR antennas very suitable for mobile applications and allows them to ensure more energetic autonomy which is always demanded in such applications.

For uncorrelated sources DoAs estimation, many high-resolution methods are adapted to the ESPAR antenna systems such as RD-MUSIC [5] and RD-ESPRIT [7, 8] and their performances are considered sufficient for DoAs estimation applications. Unfortunately, in fully or partially correlated sources situation, which is very common in communication systems (e.g. in multipath phenomenon), these methods have poor performances and their accuracy degrades severely when the rank of the data covariance matrices is affected. On the other hand, since the RD-MUSIC algorithm operates on complex baseband data, complex computation has to be executed all over the entire algorithm. Consequently, the processing time and the computational load of the DoAs estimator will be very

costly since the main computational cost of spectral MUSIC is because of the exhaustive spectral search rather than the eigen-decomposition.

In order to yield high DoAs estimation accuracy with a low computational complexity, this paper proposes three algorithms that, to the best of the authors' knowledge, have not been applied to an ESPAR antenna before. These algorithms are, respectively, the unitary RD-MUSIC algorithm, the unitary LU-RD-MUSIC algorithm and unitary QR-RD-MUSIC algorithm and are all based on real-valued representations of the estimated complex sample covariance matrices. Furthermore, since the computations of performing the unitary transformation are much less than those performing the eigen-decomposition and the search function is evaluated via real-valued matrices, the proposed unitary RD-MUSIC algorithm saves a significant amount of required computations. Therefore, the advantage is 2-fold: on the level of computation and on the level of performance. First, the computational efforts are saved because all tasks can be accomplished by real-valued computations. Thus, the calculation loads as well as the algorithm complexity are reduced by at least a factor of four since the cost of real multiplication is four times less than complex multiplication. Second, the unitary transformation improves estimator performances by an incorporated forward–backward averaging (FBA) that effectively doubles the number of samples and therefore enhances the resolution capability of DoAs estimators. As a result, two coherent or highly correlated signals can be resolved. We also demonstrate analytically and through computer simulations that, under uncorrelated signals situations, the asymptotic performances of the unitary RD-MUSIC and the FBA-RD-MUSIC algorithms are identical. Otherwise, we prove the exact equivalence of the asymptotic performance of the unitary RD-MUSIC and FBA-RD-MUSIC for uncorrelated sources situations. On the other hand, to further reduce the calculation cost and complexity without sacrificing DoAs estimation accuracy, we propose two other algorithms, namely the unitary LU-RD-MUSIC algorithm and the unitary QR-RD-MUSIC algorithm. Both of these algorithms have the advantage of requiring only linear operations and do not involve any eigen-decomposition or singular value decomposition as in common subspace-based methods. The key idea is to apply one of the real-valued orthogonal decomposition (RVOD) techniques, such as the ***QR*** decomposition or the ***LU*** decomposition, to estimate the null space basis (the noise subspace) from the estimated real-valued sample covariance matrices. These orthogonal decomposition techniques [11–13] are useful tools commonly used in linear algebra to find solutions for linear equations. Nevertheless, because both algorithms also use real-valued covariance matrices, the necessary information about the noise subspace is obtained through real-valued ***QR*** orthogonal decomposition or real-valued ***LU*** orthogonal decomposition without the loss of the advantages of the unitary RD-MUSIC algorithm mentioned above.

The outline of the paper is as follows. In Section 1, after briefly describing the ESPAR antennas signal model, we review the reactance domains (RD) technique that allows an estimation of the covariance matrix from the data available only in the output of the active element. Then, in Section 2, we explain how we can transform the complex data covariance matrix to a real-valued one. In Section 3, we develop our three proposed algorithms and we explain how we can extract the noise subspace using RVOD instead of an eigen value decomposition (EVD). The performances of the proposed methods are analysed and discussed via computer simulations in Section 4. Finally, the paper ends with some concluding comments.

In this paper, the superscripts $(.)^{\mathrm{T}}$, $(.)^{*}$, $(.)^{\mathrm{H}}$ and $(.)^{-1}$ are the matrix transpose, conjugate, hermitian and the inverse operators, respectively. $\Re(.)$ and $\Im m(.)$ denote the real-part and the imaginary-part extraction operators, respectively.

2 Problem formulation

The ESPAR antenna arrays consist of one fed active element (#0) surrounded by some parasitic radiating elements (#1 to #6) placed in the near field of the active radiator as shown in Fig. 1. The six parasitic elements are connected to the ground plane via some variable reactances $\{x_m\}_{m=1}^{M}$ whereby the radiation patterns of the ESPAR antennas can be modified by adjusting their values. We take the active element as the reference and we denote by $r = \lambda/4$ its radius and by $M = 6$ the number of the uniformly distributed parasitic elements with length $l = \lambda/4$. In the presence of K narrowband uncorrelated signals from K distinct DoAs $(\theta_1, \theta_2, \ldots, \theta_k)$ the steering matrix can be written as

$$\boldsymbol{A} = [\boldsymbol{a}(\theta_1), \boldsymbol{a}(\theta_2), \ldots, \boldsymbol{a}(\theta_k)] \tag{1}$$

where

$$\boldsymbol{a}(\theta_k) = \left[1, \mathrm{e}^{\mathrm{j}(\pi/2)\cos(\theta_k - \psi_1)}, \ldots, \mathrm{e}^{\mathrm{j}(\pi/2)\cos(\theta_k - \psi_M)}\right]^{\mathrm{T}}$$

and

$$\psi_m = \frac{2\pi}{M}(m-1); \quad \text{for } m = 1 \text{ to } M.$$

Since the data are available only in the output of the active element, an additional assumption about sources is required to form our data covariance matrix. Indeed, the K incident sources are assumed to be sent periodically from the far field. Therefore, the spatial diversity of conventional arrays is recreated by periodically changing the reactance values and, thus, the radiation patterns of the ESPAR antennas: this diversity is also called the angular diversity. While the signals are periodically sent as many times as the number of the used directional radiation patterns (e.g. $M+1$ times), the received scalar output signal from the active element $y(t_m)$

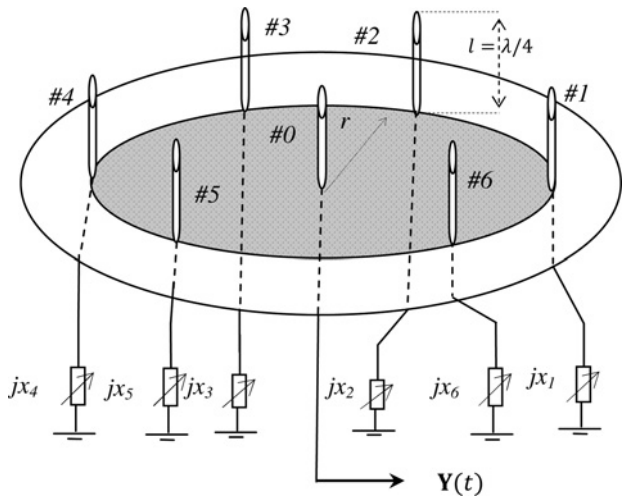

Fig. 1 *Seven elements ESPAR antennas array*

doi: 10.1049/iet-map.2011.0171

can be stocked into a vector $\boldsymbol{Y}$. By changing the reactance values of the parasitic elements under $M+1$ periods (accordingly we change the radiation pattern of the ESPAR antennas $M+1$ times), we obtain our data vector $\boldsymbol{Y}(t) \in \mathbb{C}^{(M+1)\times(1)}$. Thus, we can have several observations of the same radiated field but with different radiation patterns. This technique is known, in signal processing, as the RD technique [5].

The assumption of periodic signals allows us to write

$$S_k(t_1) = S_k(t_2) = \cdots = S_k(t_{M+1}) \tag{2}$$

where $S_k(t_m)$ is the complex magnitude of the kth incoming periodic signal at the instant time t_m.

The received signal vector $\boldsymbol{Y}(t)$ from an ESPAR antenna system can be written as

$$\boldsymbol{Y}(t) = [y(t_1), y(t_2), \ldots, y(t_M+1)]^{\mathrm{T}} \tag{3}$$

where $y(t_m) = \sum_{k=1}^{K} \boldsymbol{w}_M^{\mathrm{T}} \boldsymbol{a}(\theta_k) \boldsymbol{S}_k(t_m) + n(t_m)$

The frequency weighted matrix $\boldsymbol{W}$ is given as

$$\boldsymbol{W} = [\boldsymbol{w}_1^{\mathrm{T}}, \boldsymbol{w}_2^{\mathrm{T}}, \ldots, \boldsymbol{w}_{M+1}^{\mathrm{T}}]^{\mathrm{T}} \tag{4}$$

Each component of $\boldsymbol{W}$ is computed as

$$\boldsymbol{w}_m = 2\boldsymbol{Z}_{\mathrm{s}}(\boldsymbol{Z} + \boldsymbol{X}^{(m)})^{-1}\boldsymbol{u} \tag{5}$$

with Z_{s} is the receiver's input impedance, $\boldsymbol{u} = [1, 0, 0, \ldots, 0]^{\mathrm{T}}$, $\boldsymbol{Z} \in \mathbb{C}^{(M+1)\times(M+1)}$ is the mutual impedances matrix and $\boldsymbol{X}^{(m)}$ is a diagonal matrix that contains the $m$tth set of reactance (for $m = 1$ to $M+1$) given as

$$\boldsymbol{X}^{(m)} = \mathrm{diag}\{Z_{\mathrm{s}}, jx_1^{(m)}, jx_2^{(m)}, \ldots, jx_M^{(m)}\} \tag{6}$$

As in conventional arrays, the received data vector by the ESPAR antennas can be given in matrix notation as

$$\boldsymbol{Y}(t) = \boldsymbol{W}^{\mathrm{T}}\boldsymbol{A}\boldsymbol{S}(t) + \boldsymbol{N}(t) \tag{7}$$

The covariance matrix can be written as

$$\boldsymbol{R}_{yy} = E[\boldsymbol{Y}\boldsymbol{Y}^{\mathrm{H}}] = \boldsymbol{W}^{\mathrm{T}}\boldsymbol{A}\boldsymbol{R}_{\mathrm{s}}\boldsymbol{A}^{\mathrm{H}}\boldsymbol{W}^{*} + \boldsymbol{R}_{\mathrm{n}} \tag{8}$$

where $\boldsymbol{N}(t) = [n(t_1), n(t_2), \ldots, n(t_{M+1})]^{\mathrm{T}}$ refers to an additive Gaussian noise vector assumed to be spatially white, uncorrelated and zero mean, that is, $E[\boldsymbol{N}\boldsymbol{N}^{\mathrm{H}}] = \boldsymbol{R}_{\mathrm{n}} = \sigma^2\boldsymbol{I}$. The noise and the signals are assumed to be uncorrelated with each other (e.g. for $\forall i, j$; $E[s_i n_j^*] = 0$ and $\forall\, i \neq j$, $E[s_i s_j^*] = 0$).

With $\boldsymbol{R}_{\mathrm{s}} = E[\boldsymbol{S}\boldsymbol{S}^{\mathrm{H}}]$ denoting the signals covariance matrix, $\boldsymbol{R}_{\mathrm{n}}$ is the noise correlation matrix and σ^2 is the noise power.

The eigen-decomposition of the estimated (sample) complex covariance matrix $\widehat{\boldsymbol{R}}_{yy}$, obtained through N_{s} snapshots, can be written as

$$\widehat{\boldsymbol{R}}_{yy} = \frac{1}{N_{\mathrm{s}}}\sum_{i=1}^{N_{\mathrm{s}}} \boldsymbol{Y}\boldsymbol{Y}^{\mathrm{H}} = \widehat{\boldsymbol{E}}_{\mathrm{s}}\widehat{\boldsymbol{\Lambda}}_{\mathrm{s}}\widehat{\boldsymbol{E}}_{\mathrm{s}}^{\mathrm{H}} + \widehat{\boldsymbol{E}}_{\mathrm{n}}\widehat{\boldsymbol{\Lambda}}_{\mathrm{n}}\widehat{\boldsymbol{E}}_{\mathrm{n}}^{\mathrm{H}} \tag{9}$$

where $\widehat{\boldsymbol{E}}_s = [\widehat{\boldsymbol{e}}_1, \widehat{\boldsymbol{e}}_2, \ldots, \widehat{\boldsymbol{e}}_k]$ is the estimated complex signal subspace, $\widehat{\boldsymbol{E}}_{\mathrm{n}} = [\widehat{\boldsymbol{e}}_{k=1}, \widehat{\boldsymbol{e}}_{k+2}, \ldots, \widehat{\boldsymbol{e}}_{M+1}]$ is the estimated complex noise subspace and both $\widehat{\boldsymbol{\Lambda}}_{\mathrm{n}} = \mathrm{diag}\{\hat{\lambda}_{k+1}, \hat{\lambda}_{k+2}, \ldots, \hat{\lambda}_{M+1}\}$ and $\widehat{\boldsymbol{\Lambda}}s = \mathrm{diag}\{\hat{\lambda}_1, \hat{\lambda}_2, \ldots, \hat{\lambda}_k\}$ are diagonal matrices formed by the estimated eigenvalues $[\hat{\lambda}_1, \hat{\lambda}_2, \ldots, \hat{\lambda}_{M+1}]$ from the forward-only complex covariance matrix (9).

3 Real-valued covariance matrices

The unitary variants of subspace methods are applicable to any centro-symmetric [A simple geometrical definition is that an array is centro-symmetric if it is identical before and after rotating 180° over its centre of mass. For example, a uniform linear array is a centro-symmetric array.] array configuration. Since the ESPAR antennas shape in Fig. 1 fits this criterion, in this section we develop the unitary RD-MUSIC algorithm to benefit more advantages from ESPAR antenna systems. Hereinafter, the number of sources K is assumed to be known or has been perfectly estimated by the AIC or MDL criteria [14]. The frequency weighed matrix $\boldsymbol{W}$ is assumed full rank for the chosen reactance sets and perfectly known or obtained through experimental measurement or calculated using (5) jointly with a mutual impedance extraction technique [7]. To further simplify the exposition, some notations and definitions must be reviewed first.

We denote by $\boldsymbol{0}_{\mathrm{n}}$ the $(n \times 1)$ zero vector and we call $\boldsymbol{Q}_M \in \mathbb{C}^{M\times M}$ the left-real matrix satisfying $\boldsymbol{J}\boldsymbol{Q}_M^{*} = \boldsymbol{Q}_M$. However, we denote by $\boldsymbol{J}$ the exchange matrix, composed of ones on its anti-diagonal and zero elsewhere, given as

$$\boldsymbol{J} = \begin{bmatrix} 0 & \ldots & 0 & 1 \\ 0 & \ldots & 1 & 0 \\ \vdots & \iddots & 0 & \vdots \\ 1 & 0 & \ldots & 0 \end{bmatrix} \tag{10}$$

- An array geometry comprising sensors is called centro-symmetric if its element locations are symmetric with respect to the centre [15] and the complex radiation characteristics of paired elements are the same.
- We call the matrix $\boldsymbol{R}$ Centro-symmetric if it is symmetric about its centre. More precisely, a square matrix $\boldsymbol{R}$ is centro-symmetric when it satisfies $\boldsymbol{R}\boldsymbol{J} = \boldsymbol{J}\boldsymbol{R}$.
- We can say that $\boldsymbol{R}$ is a centro-Hermitian matrix if it satisfies $\boldsymbol{J}\boldsymbol{R}^{*}\boldsymbol{J} = \boldsymbol{R}$.

To virtually double the snapshots number and decorrelate possible correlated sources, the Centro-Hermitian property is sometimes forced by means of the so-called FBA. However, because of the specific geometry of the ESPAR antennas, components of $\widehat{\boldsymbol{R}}_{yy}$ must first be arranged to have centro-Hermitian form (linear order) as follows

$$\widehat{\boldsymbol{R}}_{\mathrm{a}} = \boldsymbol{T}\widehat{\boldsymbol{R}}_{yy}\boldsymbol{T}^{\mathrm{T}} \in \mathbb{C}^{(M+1)\times(M+1)} \tag{11}$$

where $\boldsymbol{T}$ is an $(M+1)$-by-$(M+1)$-sized transform matrix composed of zeros and ones that change the component order of $\widehat{\boldsymbol{R}}_{yy}$ into a linear order. It satisfies $\boldsymbol{T}^{\mathrm{T}}\boldsymbol{T} = \boldsymbol{I}$ and is given as

$$\boldsymbol{T} = \begin{bmatrix} 0 & 1 & 0 & 0 & 0 & 0 & 0 \\ 0 & 0 & 1 & 0 & 0 & 0 & 0 \\ 0 & 0 & 0 & 0 & 0 & 0 & 1 \\ 1 & 0 & 0 & 0 & 0 & 0 & 0 \\ 0 & 0 & 0 & 1 & 0 & 0 & 0 \\ 0 & 0 & 0 & 0 & 0 & 1 & 0 \\ 0 & 0 & 0 & 0 & 1 & 0 & 0 \end{bmatrix} \tag{12}$$

Then, instead of the conventional (forward-only) sample covariance matrix, the estimated forward–backward complex sample covariance matrix can be obtained as

$$\widehat{\boldsymbol{R}}^{\mathrm{FBA}} = \frac{1}{2}(\widehat{\boldsymbol{R}}_{\mathrm{a}} + \boldsymbol{J}\widehat{\boldsymbol{R}}_{\mathrm{a}}^{*}\boldsymbol{J}) \in \mathbb{C}^{(M+1)\times(M+1)} \tag{13}$$

The eigen-decomposition of the estimated FBA-covariance matrix $\widehat{\boldsymbol{R}}^{\mathrm{FBA}}$ (13) can be written as

$$\widehat{\boldsymbol{R}}^{\mathrm{FBA}} = \widehat{\boldsymbol{U}}_{\mathrm{s}}\widehat{\boldsymbol{\Gamma}}_{\mathrm{s}}\widehat{\boldsymbol{U}}_{\mathrm{s}}^{\mathrm{H}} + \widehat{\boldsymbol{U}}_{\mathrm{n}}\widehat{\boldsymbol{\Gamma}}_{\mathrm{n}}\widehat{\boldsymbol{U}}_{\mathrm{n}}^{\mathrm{H}} \tag{14}$$

with $\widehat{\boldsymbol{U}}_{\mathrm{s}} = [\widehat{\boldsymbol{U}}_1, \widehat{\boldsymbol{U}}_2, \ldots, \widehat{\boldsymbol{U}}_K]$ is the estimated complex signal subspace, $\widehat{\boldsymbol{U}}_{\mathrm{n}} = [\widehat{\boldsymbol{U}}_{K+1}, \widehat{\boldsymbol{U}}_{K+2}, \ldots, \widehat{\boldsymbol{U}}_{M+1}]$ is the estimated complex noise subspace and both $\widehat{\boldsymbol{\Gamma}}_{\mathrm{s}} = \mathrm{diag}\{\widehat{\gamma}_1, \widehat{\gamma}_2, \ldots, \widehat{\gamma}_K\}$ and $\widehat{\boldsymbol{\Gamma}}_{\mathrm{n}} = \mathrm{diag}\{\widehat{\gamma}_{K+1}, \widehat{\gamma}_{K+2}, \ldots, \widehat{\gamma}_{M+1}\}$ are diagonal matrices formed by the estimated eigenvalues $[\widehat{\gamma}_1, \widehat{\gamma}_2, \ldots, \widehat{\gamma}_{M+1}]$.

Since the inner product between any two conjugate centro-symmetric vectors is real valued, any matrix of which each row is conjugate centro-symmetric may be employed to transform the complex-valued element into a real-valued manifold. As noted by numerous authors [16–19], the simplest matrix for accomplishing that is $\boldsymbol{Q}_M$ defined as follows

$$\boldsymbol{Q}_M = \begin{cases} \dfrac{1}{\sqrt{2}}\begin{bmatrix} \boldsymbol{I}_{(M-1/2)} & \boldsymbol{0}_{(M-1/2)} & j\boldsymbol{I}_{(M-1/2)} \\ \boldsymbol{0}^{\mathrm{T}}_{(M-1/2)} & \sqrt{2} & \boldsymbol{0}^{\mathrm{T}}_{(M-1/2)} \\ \boldsymbol{J}_{(M-1/2)} & \boldsymbol{0}_{(M-1/2)} & -j\boldsymbol{J}_{(M-1/2)} \end{bmatrix}, & \text{for odd } M \\ \dfrac{1}{\sqrt{2}}\begin{bmatrix} \boldsymbol{I}_{(M/2)} & j\boldsymbol{I}_{(M/2)} \\ \boldsymbol{J}_{(M/2)} & -j\boldsymbol{J}_{(M/2)} \end{bmatrix}, & \text{for even } M \end{cases} \tag{15}$$

We introduce, then, the real-valued covariance matrix [20] as

$$\boldsymbol{R}_{\mathrm{u}} = \boldsymbol{Q}_{M+1}^{\mathrm{H}}\boldsymbol{R}^{\mathrm{FBA}}\boldsymbol{Q}_{M+1} \tag{16}$$

The real-valued sample covariance matrix can be given as

$$\widehat{\boldsymbol{R}}_{\mathrm{u}} = \frac{1}{2}(\boldsymbol{Q}_{M+1}^{\mathrm{H}}\widehat{\boldsymbol{R}}_{\mathrm{a}}\boldsymbol{Q}_{M+1} + \boldsymbol{Q}_{M+1}^{\mathrm{H}}\boldsymbol{J}\widehat{\boldsymbol{R}}_{\mathrm{a}}^{*}\boldsymbol{J}\boldsymbol{Q}_{M+1}) \tag{17}$$

Using the fact that $\boldsymbol{J}\boldsymbol{Q}_{M+1}^{*} = \boldsymbol{Q}_{M+1}$ and $\boldsymbol{J}^{\mathrm{H}} = \boldsymbol{J}$, (17) becomes

$$\widehat{\boldsymbol{R}}_{\mathrm{u}} = \frac{1}{2}(\boldsymbol{Q}_{M+1}^{\mathrm{H}}\widehat{\boldsymbol{R}}_{\mathrm{a}}\boldsymbol{Q}_{M+1} + (\boldsymbol{Q}_{M+1}^{\mathrm{H}})^{*})^{\mathrm{H}}\widehat{\boldsymbol{R}}_{\mathrm{a}}^{*}\boldsymbol{Q}_{M+1}^{*}) \tag{18}$$

From (18), we show that matrix $\widehat{\boldsymbol{R}}_{\mathrm{u}}$ can be directly estimated from the forward-only sample covariance matrix as

$$\widehat{\boldsymbol{R}}_{\mathrm{u}} = \Re\{\boldsymbol{Q}_{M+1}^{\mathrm{H}}\widehat{\boldsymbol{R}}_{\mathrm{a}}\boldsymbol{Q}_{M+1}\} \in \mathbb{R}^{(M+1)\times(M+1)} \tag{19}$$

Equation (18) forms the basis for the application of all our proposed unitary RD-MUSIC algorithms and all computations can now be done with real-valued matrices. Based on (18) and (19), it can be readily shown that the FBA is achieved by transforming the complex components of the covariance matrix $\widehat{\boldsymbol{R}}_{yy}$ into a real-valued one $\widehat{\boldsymbol{R}}_{\mathrm{u}}$ after the arrangement of their components into linear form according to (11). Moreover, since (18) proves that the real-valued covariance matrix estimated from the forward-only covariance matrix is equivalent to those estimated from the FBA covariance matrix (14), our proposed algorithms can be applied to coherent sources scenarios. In addition, estimating the real-valued covariance matrix through the forward-only covariance matrix not only yields to a very low computational cost with a reduced data storage requirements, but also, it avoids certain degradations of asymptotic performances caused by the FBA technique [20].

4 Development of the proposed methods

4.1 Unitary RD-MUSIC algorithm

Let us now formulate the unitary RD-MUSIC algorithm that is basically related to the centro-symmetry propriety of the used ESPAR antennas shape. It begins with the estimation of the sample covariance matrix $\widehat{\boldsymbol{R}}_{yy}$ according to (9). Then, similar to standard MUSIC [1], the real-valued noise subspace $\widehat{\boldsymbol{E}}_{\mathrm{s}}^{\mathrm{r}}$ can be computed via real-valued eigen-decomposition of the covariance matrix (19). Therefore the next step is to estimate the real-valued noise subspace as the $(M+1-K)$ real eigenvectors corresponding to the $(M+1-K)$ smallest real eigenvalues of $\widehat{\boldsymbol{R}}_{\mathrm{u}}$ as

$$\widehat{\boldsymbol{R}}_{\mathrm{u}} = \widehat{\boldsymbol{E}}_{\mathrm{s}}^{\mathrm{r}}\widehat{\boldsymbol{\Lambda}}_{\mathrm{s}}^{\mathrm{r}}\widehat{\boldsymbol{E}}_{\mathrm{s}}^{\mathrm{r}^{\mathrm{H}}} + \widehat{\boldsymbol{E}}_{\mathrm{n}}^{\mathrm{r}}\widehat{\boldsymbol{\Lambda}}_{\mathrm{n}}^{\mathrm{r}}\widehat{\boldsymbol{E}}_{\mathrm{n}}^{\mathrm{r}^{\mathrm{H}}} \tag{20}$$

where $\widehat{\boldsymbol{E}}_{\mathrm{s}}^{\mathrm{r}} = [\hat{\boldsymbol{e}}_1^{\mathrm{r}}, \hat{\boldsymbol{e}}_2^{\mathrm{r}}, \ldots, \hat{\boldsymbol{e}}_K^{\mathrm{r}}]$ is the estimated real-valued signal subspace, $\widehat{\boldsymbol{E}}_{\mathrm{n}}^{\mathrm{r}} = [\hat{\boldsymbol{e}}_{k+1}^{\mathrm{r}}, \hat{\boldsymbol{e}}_{k+2}^{\mathrm{r}}, \ldots, \hat{\boldsymbol{e}}_{M+1}^{r}]$ is the estimated real-valued noise subspace and both $\widehat{\boldsymbol{\Lambda}}_{\mathrm{s}}^{\mathrm{r}} = \mathrm{diag}\{\hat{\lambda}_1^{\mathrm{r}}, \hat{\lambda}_2^{\mathrm{r}}, \ldots, \hat{\lambda}_K^{\mathrm{r}}\}$ and $\widehat{\boldsymbol{\Lambda}}_{\mathrm{s}}^{\mathrm{r}} = \mathrm{diag}\{\hat{\lambda}_{k+1}^{\mathrm{r}}, \hat{\lambda}_{k+2}^{\mathrm{r}}, \ldots, \hat{\lambda}_{M+1}^{\mathrm{r}}\}$ are real-valued diagonal matrices formed by the estimated eigenvalues $[\hat{\lambda}_1^{\mathrm{r}}, \hat{\lambda}_2^{\mathrm{r}}, \ldots, \hat{\lambda}_{M+1}^{\mathrm{r}}]$.

On the other hand, it can be seen that both eigenvectors and eigenvalues of matrices (19) and (14) are related to those of matrix (9) as follows

$$\widehat{\boldsymbol{E}}^{\mathrm{r}} = \boldsymbol{Q}_{M+1}^{\mathrm{H}}\boldsymbol{T}\widehat{\boldsymbol{E}} \tag{21}$$

$$\widehat{\boldsymbol{\Lambda}}^{\mathrm{r}} = \boldsymbol{Q}_{M+1}^{\mathrm{H}}\boldsymbol{T}\widehat{\boldsymbol{\Lambda}} \tag{22}$$

$$\widehat{\boldsymbol{U}} = \boldsymbol{T}\widehat{\boldsymbol{E}} \tag{23}$$

$$\widehat{\boldsymbol{\Gamma}} = \boldsymbol{T}\widehat{\boldsymbol{\Lambda}} \tag{24}$$

Finally, as any MUSIC-type algorithm, the estimated DoAs are taken as the directions (θ) that maximise a spectrum search function. Starting with the RD-MUSIC algorithm the search function is given as

$$P_{\mathrm{MUSIC}}^{\mathrm{ESPAR}} = ((\boldsymbol{W}^{\mathrm{T}}\boldsymbol{a}(\theta_k))^{\mathrm{H}}\widehat{\boldsymbol{E}}_{\mathrm{n}}\widehat{\boldsymbol{E}}_{\mathrm{n}}^{\mathrm{H}}\boldsymbol{W}^{\mathrm{T}}\boldsymbol{a}(\theta_k))^{-1} \tag{25}$$

Based on (23) and (24), the FBA-RD-MUSIC search function can be written as

$$P_{\mathrm{FBA\text{-}MUSIC}}^{\mathrm{ESPAR}} = ((\boldsymbol{T}\boldsymbol{W}^{\mathrm{T}}\boldsymbol{a}(\theta_k))^{\mathrm{H}}\widehat{\boldsymbol{U}}_{\mathrm{n}}\widehat{\boldsymbol{U}}_{\mathrm{n}}^{\mathrm{H}}\boldsymbol{T}\boldsymbol{W}^{\mathrm{T}}\boldsymbol{a}(\theta_k))^{-1} \tag{26}$$

By using the fact that $\boldsymbol{Q}_{M+1}\boldsymbol{Q}_{M+1}^{\mathrm{H}} = \boldsymbol{I}$, (26) becomes

$$P_{\mathrm{FBA\text{-}MUSIC}}^{\mathrm{ESPAR}} = ((\boldsymbol{T}\boldsymbol{W}^{\mathrm{T}}\boldsymbol{a}(\theta_k))^{\mathrm{H}}\boldsymbol{Q}_{M+1}\boldsymbol{Q}_{M+1}^{\mathrm{H}} \times \widehat{\boldsymbol{U}}_{\mathrm{n}}\widehat{\boldsymbol{U}}_{\mathrm{n}}^{\mathrm{H}}\boldsymbol{Q}_{M+1}\boldsymbol{Q}_{M+1}^{\mathrm{H}}\boldsymbol{T}\boldsymbol{W}^{\mathrm{T}}\boldsymbol{a}(\theta_k))^{-1} \tag{27}$$

Using (21) and (22) and through some mathematical manipulations, the unitary RD-MUSIC search function can

doi: 10.1049/iet-map.2011.0171

be given as

$$P^{\text{ESPAR}}_{\text{Unit-MUSIC}} = (\tilde{\boldsymbol{a}}(\theta_k)^{\text{H}}\widehat{\boldsymbol{E}}^{\text{r}}_{\text{n}}\widehat{\boldsymbol{E}}^{\text{r}^{\text{H}}}_{\text{n}}\tilde{\boldsymbol{a}}(\theta_k))^{-1} \tag{28}$$

Note that the real-valued RD-steering vector given as: $\tilde{\boldsymbol{a}}(\theta_k) = \boldsymbol{Q}^{\text{H}}_{M+1}(\boldsymbol{T}\boldsymbol{W}^{\text{T}}\boldsymbol{a}(\theta_k))$ is orthogonal to the columns of the real-valued noise subspace matrix $\boldsymbol{E}^{\text{r}}_{\text{n}}$ and proportional to the columns of the real-valued signal subspace $\boldsymbol{E}^{\text{r}}_{\text{s}}$. We stress also that, since the unitary RD-MUSIC algorithm search function operates on real-valued data and the eigen-decomposition is computed for real-valued matrices instead of complex-valued matrices, the calculation complexity and the processing time of the proposed algorithm are about four times lower than the RD-MUSIC [5]. Therefore our unitary RD-MUSIC algorithm can be considered as a good candidate for real-time implementation.

4.2 Unitary RD-MUSIC algorithm with RVOD

The classic MUSIC algorithm [1] is based on the orthogonality between the noise and the signal subspaces estimated through an eigen-decomposition of the data covariance matrix. In this sub-section, we will demonstrate that these subspaces can be estimated through only linear operations. Based on some orthogonal decomposition techniques, such as the $\boldsymbol{LU}$ decomposition and the $\boldsymbol{QR}$ decomposition, an estimation of the orthonormal vectors that span the same subspaces spanned by the columns (e.g. basis of the noise subspace) of the sample covariance matrix can be achieved. Therefore the complexity of the DoAs estimator is further reduced since the use of the standard EVD technique has been avoided. The $\boldsymbol{LU}$ decomposition involves that the real-valued matrix $\boldsymbol{R}_{\text{u}}$ in (20) can be expressed as the product of two real matrices: an orthogonal $(M+1)$-order square matrix $\boldsymbol{L}$ and an $(M+1)$-order square upper triangular matrix $\boldsymbol{U}$. Thus, the $\boldsymbol{LU}$ decomposition of $\boldsymbol{R}_{\text{u}}$ can be written as

$$\boldsymbol{LU}_{(\boldsymbol{R}_{\text{u}})} = \boldsymbol{LU} = [\boldsymbol{L}_1\boldsymbol{L}_2]\begin{bmatrix}\boldsymbol{U}_{11} & \boldsymbol{U}_{12}\\ \boldsymbol{0}_{M-K+1} & \boldsymbol{U}_{22}\end{bmatrix} \tag{29}$$

where $\boldsymbol{U}_{11} \in \mathbb{R}^{K\times K}$, $\boldsymbol{U}_{22} \in \mathbb{R}^{(M-K+1)\times(M-K+1)}$ are both real-valued upper triangular matrices and $\boldsymbol{U}_{12} \in \mathbb{R}^{(K)\times(M-K+1)}$ is a real-valued matrix.

Furthermore, since the sub-matrix $\boldsymbol{U}_{22}$ has a small norm, we can easily extract the basis of the noise sub-space from

$$\widetilde{\boldsymbol{U}} = [\boldsymbol{U}_{11}\ \boldsymbol{U}_{12}] \tag{30}$$

Let $\boldsymbol{p} = [\boldsymbol{p}_1\ \boldsymbol{p}_2]^{\text{T}}$, with $\boldsymbol{p}_1 \in \mathbb{R}^{(K\times 1)}$ and $\boldsymbol{p}_2 \in \mathbb{R}^{((M-K+1)\times 1)}$, be any vector belonging to the null subspace of the real-valued matrix $\widetilde{\boldsymbol{U}}$ which is also the null space of the real-valued covariance matrix $\boldsymbol{R}_{\text{u}}$. Therefore we can write

$$\widehat{\boldsymbol{R}}_{\text{u}}\,\boldsymbol{p} = 0 \tag{31}$$

Substituting (29) and (30) in (31) yields to

$$[\boldsymbol{L}_1][\boldsymbol{U}_{11}\quad \boldsymbol{U}_{12}]\begin{bmatrix}\boldsymbol{p}_1\\ \boldsymbol{p}_2\end{bmatrix} = 0 \tag{32}$$

Equation (32) implies that

$$\boldsymbol{U}_{12}\,\boldsymbol{p}_1 + \boldsymbol{U}_{12}\,\boldsymbol{p}_2 = 0 \tag{33}$$

Then, since $\boldsymbol{U}_{11}$ is a non-singular matrix with full rank (i.e. $\text{rank}(\boldsymbol{U}_{11}) = K$), $\boldsymbol{p}_1$ can be given as a function of $\boldsymbol{p}_2$ as follows

$$\boldsymbol{p}_1 = -\boldsymbol{U}^{-1}_{11}\boldsymbol{U}_{12}\,\boldsymbol{p}_2 \tag{34}$$

Based on (34), $\boldsymbol{p}$ can be written as

$$\boldsymbol{p} = \begin{bmatrix}\boldsymbol{p}_1\\ \boldsymbol{p}_2\end{bmatrix} = \begin{bmatrix}-\boldsymbol{U}^{-1}_{11}\boldsymbol{U}_{12}\\ \boldsymbol{I}_{M-K+1}\end{bmatrix}\boldsymbol{p}_2 = \boldsymbol{E}_{\boldsymbol{LU}}\boldsymbol{p}_2 \tag{35}$$

Substituting (35) into (31) yields

$$\boldsymbol{R}_{\text{u}}\,\boldsymbol{p} = \boldsymbol{R}_{\text{u}}\boldsymbol{E}_{\boldsymbol{LU}}\,\boldsymbol{p}_2 = 0 \tag{36}$$

or simply

$$\boldsymbol{R}_{\text{u}}\boldsymbol{E}_{\boldsymbol{LU}} = 0 \tag{37}$$

Finally, the null space of $\boldsymbol{R}_{\text{u}}$ can be estimated as

$$\boldsymbol{E}_{\boldsymbol{LU}} = \begin{bmatrix}-\boldsymbol{U}^{-1}_{11}\boldsymbol{U}_{12}\\ \boldsymbol{I}_{M-K+1}\end{bmatrix} \tag{38}$$

Equation (37) proves that the necessary information about the noise subspaces can be extracted using the RVOD. However, although the null spaces in (38) and in (21) have the same form and dimensions, the columns of $\boldsymbol{E}_{\boldsymbol{LU}}$ are not orthonormal as those provided by the standard EVD. To achieve better results and enhance the numerical stability of our proposed algorithms, we make the basis of the estimated null space of $\widehat{\boldsymbol{E}}_{\boldsymbol{LU}}$ orthonormal by forming an orthogonal projection onto this subspace as follows

$$\widehat{\boldsymbol{E}}_{\text{OD}} = \widehat{\boldsymbol{E}}_{\boldsymbol{LU}}(\widehat{\boldsymbol{E}}^{\text{H}}_{\boldsymbol{LU}}\widehat{\boldsymbol{E}}_{\boldsymbol{LU}})^{-1}\widehat{\boldsymbol{E}}^{\text{H}}_{\boldsymbol{LU}} \tag{39}$$

The real-valued $\boldsymbol{QR}$ orthogonal decomposition is done in the same way as described for the real-valued $\boldsymbol{LU}$ decomposition derived above. Thus, the search function of both unitary RD-MUSIC algorithms based on RVOD techniques can be given as

$$P^{\text{ESPAR}}_{\text{unit-RVOD-MUSIC}} = (\tilde{\boldsymbol{a}}(\theta_k)^{\text{H}}\widehat{\boldsymbol{E}}_{\text{OD}}\tilde{\boldsymbol{a}}(\theta_k))^{-1} \tag{40}$$

In comparison between these two RVOD methods, it is interesting to point out here that the $\boldsymbol{LU}$ orthogonal decomposition [11] can reduce the calculation complexity over the $\boldsymbol{QR}$ decomposition by a factor of two. More precisely, the number of additions and multiplications required by the $\boldsymbol{QR}$ decomposition is about twice that of using the $\boldsymbol{LU}$ decomposition. On the other hand, no more digits are required in inexact arithmetic because the numerical stability of the $\boldsymbol{QR}$ decomposition is guaranteed which reduces the need to a large memory capacity to store the data.

5 Cramer Rao bound (CRB)

The CRB is defined as the ultimate accuracy achieved by any unbiased estimator: $E(\hat{\theta}_i - \theta_i) \geq \text{CRB}(\hat{\theta}_i)$ for the ith signal where $\hat{\theta}_i$ is the estimated value of DoA θ_i. Thus, to evaluate performances on DoAs estimation of the proposed algorithms through computer simulation, an analytical CRB expression that takes into account such effects is required. Since the frequency weight matrix $\boldsymbol{W}$ is independent of the

sources DoAs and assumed to be a constant matrix, it can be included in the CRB derivations by replacing the conventional steering matrix $\boldsymbol{A}$ by the new RD-steering matrix $\boldsymbol{A}_e = \boldsymbol{W}^T\boldsymbol{A}$. In [21], an expression for the CRB was derived for conventional antennas array systems and can also be applied to the ESPAR antenna by changing the steering matrix. This expression is given as

$$\text{CRB} = \frac{\sigma^2}{2N_s}[(\text{Real}\{(\boldsymbol{D}^H\boldsymbol{P}_e^{\pm}\boldsymbol{D}) \odot \boldsymbol{R}_s^T\})^{-1}]_{ii} \qquad (41)$$

Here, $\odot$ denotes the Hadamard product and $\boldsymbol{P}_e^{\pm}$ is the orthogonal projector on the null space of $\boldsymbol{A}_e$ expressed as

$$\boldsymbol{P}_e^{\pm} = \boldsymbol{I}_{M+1} - \boldsymbol{A}_e(\boldsymbol{A}_e^H\boldsymbol{A}_e)^{-1}\boldsymbol{A}_e^H.$$

where $\boldsymbol{I}_{M+1}$ is the identity matrix and $\boldsymbol{D} = \boldsymbol{W}^T\dfrac{\partial \boldsymbol{A}}{\partial \theta}$.

6 Simulation results

In this sub-section, we conduct computer simulations to evaluate the performances of our three proposed algorithms and compare them with both the RD-MUSIC algorithm [5] and conventional antenna arrays. In the first part, it will be of our interest to validate our approach by studying the precision and the resolution capabilities of these algorithms under uncorrelated sources scenarios. After that, we will perform other simulations under correlated sources situations to demonstrate the efficiency of these algorithms in such a scenario.

6.1 Performances on DoAs estimation under uncorrelated sources

This first simulation, shown in Fig. 2, proves the multiple-signal-resolution capability of the proposed methods. It depicts the resulting MUSIC spectra, these being the unitary RD-MUSIC (dotted line), the unitary LU-RD-MUSIC (dashed line) and the RD-MUSIC algorithm (solid line), obtained through 2000 snapshots to compute $\widehat{\boldsymbol{R}}_u$ from (19) and 500 simulation trials when three uncorrelated sources impinge the ESPAR antennas from 25, 55 and 80°, respectively with an signal to noise ratio (SNR) level of 35 dB. In Fig. 2, the unitary QR-RD-MUSIC spectrum is not plotted because of the similarity to the unitary LU-RD-MUSIC spectrum. We can clearly see that, in comparison with the unitary RD-MUSIC, the unitary LU-RD-MUSIC spectrum has more selective peaks towards the true DoAs. Thus, we can say that the RVOD techniques can efficiently extract the basis of the noise subspace from the real-valued sample covariance matrices and achieve satisfactory results in DoAs estimation.

Lets us now study the precision in DoAs estimation of these various methods. For this purpose we use, as performance parameters, the root mean square error (RMSE) defined as $\text{RMSE}(\hat{\theta}_k) = \sqrt{\dfrac{1}{N_s}\sum_{n=1}^{N_s}(\hat{\theta}_k - \hat{\theta}_k)^2}$ and the RD-CRB standard deviation given by $\text{Std}_{\text{RD-CRB}}(\hat{\theta}) = \sqrt{\text{CRB}(\hat{\theta}_i)}$.

The simulation shown in Fig. 3 aims at investigating the performances of the proposed methods and comparing it with the Std-RD-CRB. The angular resolution capabilities are illustrated against the angular separation $\Delta\theta = |\theta_2 - \theta_1|$ between two incoming uncorrelated sources. The first source has a DoA at θ_1 that increases from 65 to 90°, however, the second source has a fixed DoA at $\theta_2 = 60°$ and only the first source RMSE curve is shown since the other curve will behave similarly. As mentioned above, the exact equivalence between the unitary RD-MUSIC and FB-RD-MUSIC algorithms is clearly shown in Fig. 3 since their RMSE curves are identical. Results in Fig. 3 also show that the unitary LU-RD-MUSIC performs better DoAs estimation accuracy even for a very close source' DoAs ($\Delta\theta = 5°$) and its RMSE curve is closer to the Std-CRB for a large sources angular separation ($\Delta\theta > 25°$). Thus, in comparison with other methods, the unitary RVOD-RD-MUSIC exhibits better estimation errors and can perform robust DoAs estimation even when the incoming sources are closer together.

To further validate our approach, we compare the performances on DoAs estimation of these methods

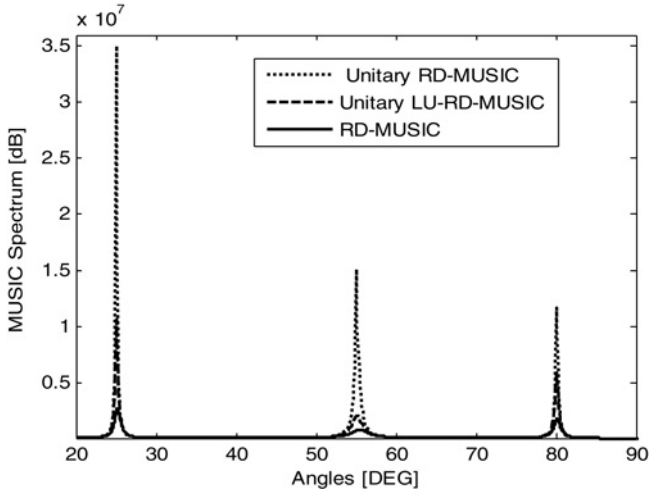

Fig. 2 *Resulting MUSIC spectrums of the proposed algorithms as a function of azimuth angles: three uncorrelated sources incoming from 25, 55 and 80°, respectively. Each source has an SNR = 35 dB where 2000 snapshots are used to compute $\widehat{\boldsymbol{R}}_u$ from (19) with 500 simulation trials*

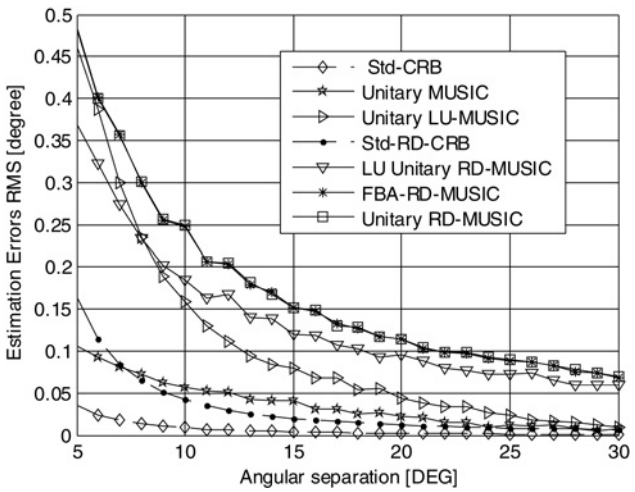

Fig. 3 *DoAs estimation errors (RMSE) against the angular separation between two incoming uncorrelated sources from 60° and 60° + Δθ, respectively. SNR is set to 35 dB, 2000 snapshots are used to estimate both $\widehat{\boldsymbol{R}}_{FBA}$ and $\widehat{\boldsymbol{R}}_u$ from (13) and (19), respectively, with 500 independent trials run*

doi: 10.1049/iet-map.2011.0171

achieved with ESPAR antennas to those obtained with conventional antennas arrays. The conventional array is assumed to be perfectly calibrated, so, mutual coupling effects because of $r = \lambda/4$ may be neglected. Simulations in Fig. 3 show that conventional array antenna gives better results than ESPAR antennas. However, although such results could be expected, performances of ESPAR antennas can be considered sufficient for DoAs estimation applications in comparison with conventional arrays (less than 0.1° for $\Delta\theta < 20^\circ$). On the other hand, the cost reduction using only a single active receiver as well as the low power consumption of ESPAR antennas, may outweigh their loss of performances compared to conventional arrays.

Since the number of snapshots (samples) is an important criterion in real-time implementation, in practice we want to decrease the calculation cost and the time processing of the DoAs estimators as much as possible by working with a small snapshots number. As all proposed algorithms are based on the unitary transformation, in which the number of snapshots virtually increases, it yields better results in few snapshots scenario compared to the RD-MUSIC. To clearly appreciate the influence of the snapshots number on the performances of the proposed algorithms we summarise, in Table 1, the DoAs estimation values of two incoming uncorrelated signals from 55 and 90°, respectively, obtained through 500 simulation trials with an SNR level of 25 dB. The main goal of those results is to highlight the improvement brought by the proposed algorithms over the RD-MUSIC in few snapshots number scenarios. We can see from the precision on DoAs estimation that our methods remain good for a small number of snapshots. By 50 snapshots we reach an estimation error of 0.6° that decreases to 0.1° when the snapshots number increases to 2000. Therefore our approach can be considered usable for DoAs estimation even with a reduced number of samples since it performs better finite sample performance than the RD-MUSIC algorithm.

6.2 Performances on DoAs estimation of correlated sources

In the previous part, we have verified that all our proposed methods can be used for DoAs estimation applications. In this second part, our interest is to study their DoAs estimation capabilities against the absolute value of the sources' correlation coefficient $|\rho|$.

The simulation shown in Fig. 4 aims at demonstrating the accuracy on DoAs estimation of our proposed algorithm under correlated sources situation. It depicts the resulting RMSE of DoAs estimation computed using 1000 snapshots and averaged over 500 simulation trials against the correlation coefficient between two correlated sources impinging the ESPAR antenna from 30 and 80°, respectively, with an SNR = 30 dB. Again, we have not included the results for the second source because of the similarity and we focus only on the RMSE of source incoming from 30°. We show that both unitary RD-MUSIC and unitary LU-RD-MUSIC algorithms can prominently distinguish the DoAs and perform significant performances improvement on DoAs estimation over the RD-MUSIC algorithm. Moreover, Fig. 4 illustrates a sensitive improvement on DoAs estimation with the unitary LU-RD-MUSIC for highly correlated sources scenarios ($|\rho| < 0.85$) over the unitary RD-MUSIC.

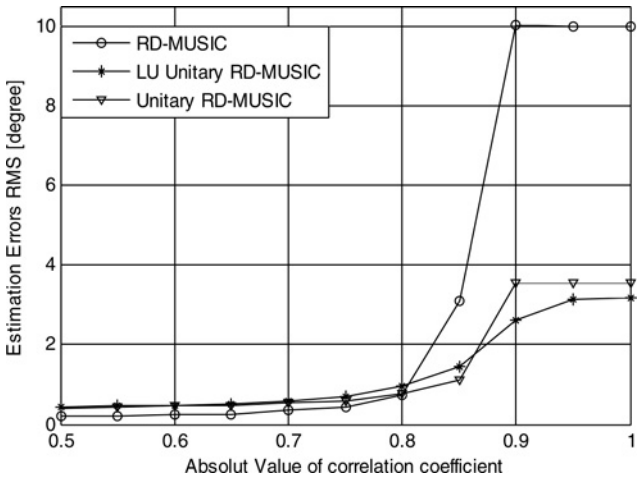

Fig. 4 *Resulting RMSE of DoAs estimation against the sources correlation coefficient: sources incoming from 30 and 80°, SNR = 30 dB, 1000 snapshots and 500 simulation trials*

Since Fig. 4 clearly indicates that, under correlated sources situations and for large SNR levels, both unitary RVOD-RD-MUSIC algorithms can provide better results, it is interesting to compare their performances in such a scenario. For this purpose, Fig. 5 illustrates the resulting RMSE on DoAs estimation computed using 5000 snapshots and averaged over 2000 simulation trials against the absolute values of correlation coefficient between two correlated sources that impinge the ESPAR antenna from the same DoAs as in the previous simulation but with an SNR = 35 dB.

As with the results given in Fig. 4, only the behaviour of the incoming source from 30° is shown. Results given in Fig. 5 will be interpreted with respect to three cases: uncorrelated sources, moderately correlated sources and fully correlated sources situations. Under uncorrelated sources situation, we show that all algorithms can ensure an accurate DoAs estimation and behave approximately in the same way. However, as soon as the sources become moderately correlated ($0.2 \leq |\rho| \leq 0.65$), in contrast to the unitary RD-MUSIC that still gives an accurate DoAs estimation, we show some degradations in the performances achieved by both unitary RVOD-RD-MUSIC algorithms.

Table 1 Influence of the snapshots number on DoAs estimation

	Unitary LU-RD-MUSIC		Unitary QR-RD-MUSIC		Unitary RD-MUSIC		RD-MUSIC	
SNR, dB	25	25	25	25	25	25	25	25
true DoAs, DEG	55°	90°	55°	90°	55°	90°	55°	90°
estimated DoAs for 50 snapshots	54.7°	90.6°	54.7°	90.5°	54.8°	90.6°	54.6°	90.8°
estimated DoAs for 200 snapshots	54.6°	90.3°	54.6°	90.3°	55.2°	90.4°	55.3°	90.5°
estimated DoAs for 2000 snapshots	55.1°	90.2°	55.1°	90.2°	55.1°	90.3°	55.2°	90.4°

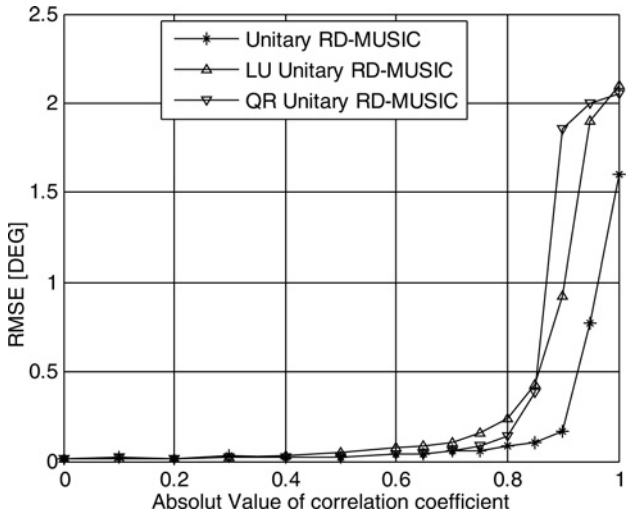

Fig. 5 *RMSE of DoAs estimation against the sources correlation coefficient: sources incoming from 30 and 80°, SNR = 35 dB, 5000 snapshots and 2000 simulation trials*

In the last case, where the sources are fully correlated (i.e. $0.9 \leq |\rho|$), both RVOD-based unitary RD-MUSIC algorithms have a sensitive failure on DoAs estimation. This may be due to the fact that the sources correlation affects the data covariance matrices rank and therefore it becomes difficult to extract the noise sub-space basis through the RVOD techniques. This can be further verified by analysing the behaviour of the unitary RD-MUSIC that is based on the standard EVD to estimate the noise sub-space. Indeed, as illustrated in Fig. 5, the unitary RD-MUSIC algorithm shows acceptable results for DoAs estimation (RMSE less than 0.8°) for an important sources correlation coefficient ($|\rho| = 0.95$), however, an important estimation errors (RMSE more than 1.5°) is shown when the incoming sources are coherent ($|\rho| = 1$). Thus, in comparison with the standard EVD, Fig. 5 clearly indicates that both proposed RVOD techniques are unable to achieve an accurate estimation of the noise sub-space except when the incoming sources are coherent as it is also the case for the unitary RD-MUSIC. Nonetheless, the gain in computational load provided by these techniques, by using only linear operations, may overcome their performance loss in coherent sources situation.

7 Concluding comments

Based on unitary formulation of the MUSIC algorithm for ESPAR antennas, we have proposed three algorithms to estimate the DoAs of impinging highly correlated signals. These algorithms are based on real-valued transformation of the estimated covariance matrices. The real-valued transformation not only yields higher-resolution capabilities, but also considerably reduces the estimator computational complexity, the required capacity to store the data as well as the processing time which is a challenging criterion for a real-time implementation of any DoAs estimator (e.g. as on a DSP chip). To ensure more calculation complexity reductions, two RVOD techniques are introduced to estimate the real-valued noise subspaces instead of the standard EVD ones. From the simulation results, we can see that, under highly correlated sources, the proposed algorithms can prominently distinguish the DoAs and perform significant improvement on DoAs estimation over the RD-MUSIC algorithm. In the same way, we demonstrate that the ***LU*** decomposition can perform sensitive improvements on DoAs estimation over the ***QR*** decomposition especially under highly correlated sources environment.

8 Acknowledgment

The authors gratefully acknowledge the contributions of reviewers and thank the anonymous reviewers for their valuable comments that significantly improved the quality of this paper.

9 References

1 Schmit, O.R.: 'Multiple emitter location and signal parameters estimation', *IEEE Trans. Antennas Propag.*, 1986, **34**, pp. 276–280
2 Marcos, S., Marsal, A., Benidir, M.: 'The propagator method for source bearing estimation', *Signal Process. Elsevier*, 1995, **42**, pp. 121–138
3 Harabi, F., Changuel, H., Gharsallah, A.: 'Estimation of 2-D direction of arrival with an extended correlation matrix'. IEEE Workshop on Positioning, Navigation and Communication, Hanover, March 2007
4 Harabi, F., Changuel, H., Gharsallah, A.: 'A new estimation of direction of arrival algorithm with a special antennas shape', *Smart Mater. Struct. J. (SMS)*, 2007, **16**, pp. 2595–2599
5 Plapous, C., Cheng, J., Taillefer, E., Hirata, A., Ohira, T.: 'Reactance domain MUSIC algorithm for electronically steerable parasitic array radiator antenna', *IEEE Trans. Antenna Propag.*, 2004, **52**, (12), pp. 3257–3264
6 Taillefer, E., Hirata, A., Ohira, T.: 'Direction-of-arrival estimation using radiation power pattern with an ESPAR antenna', *IEEE Trans. Antenna Propag.*, 2005, **53**, (11), pp. 3486–3495
7 Taillefer, E., Hirata, A., Ohira, T.: 'Reactance-domain ESPRIT algorithm for a hexagonally shaped seven-element ESPAR antenna', *IEEE Trans. Antenna Propag.*, 2005, **53**, (11), pp. 3486–3495
8 Taillefer, E., Nomura, W., Cheng, J., Taromaru, M., Watanabe, Y., Ohira, T.: 'Enhanced reactance-domain ESPRIT algorithm employing multiple beams and translational-invariance soft selection for direction-of-arrival estimation in the full azimuth', *IEEE Trans. Antennas Propag.*, 2008, **56**, (8), pp. 2514–2526
9 Hirata, A., Taillefer, E., Yamada, H., Ohira, T.: 'Handheld direction of arrival finder with electronically steerable parasitic array radiator using the reactance-domain MUltiple SIgnal Classification algorithm', *IET Microw. Antennas Propag.*, 2007, **1**, (4), pp. 815–821
10 Taillefer, E., Cheng, J., Watanabe, Y.: 'Full azimuth direction-of-arrival estimation with successive-selection technique', *IEEE Trans. Signal Process.*, 2008, **56**, (12), pp. 5903–5915
11 Fargues, M.P., Ferreira, M.P.: 'Investigations in the numerical behavior of the adaptive rank-revealing *QR* factorization', *IEEE Trans. Acoust. Speech Signal Process.*, 1995, **43**, pp. 2787–2791
12 Bischof, C.H., Shroff, G.M.: 'On updating signal subspaces', *IEEE Trans. Acoust. Speech Signal Process.*, 1992, **40**, pp. 96–105
13 Miranian, L., Gu, M.: 'Strong rank revealing LU factorizations', *Linear Algebr. Appl.*, 2003, **367**, pp. 1–16
14 Wax, M., Kailath, T.: 'Detection of signals by information theoretic criteria', *IEEE Trans. Acoust. Speech Signal Process.*, 1985, **33**, pp. 387–392
15 Thakre, A., Haardt, M., Giridhar, K.: 'Single snapshot spatial smoothing with improved effective array aperture', *IEEE Signal Process. Lett.*, 2009, **16**, (6), pp. 505–508
16 Haardt, M., Nossek, J.A.: 'Unitary ESPRIT: how to obtain increased estimation accuracy with a reduced computational burden', *IEEE Trans. Signal Process.*, 1995, **43**, (5), pp. 1232–1242
17 Hnarng, K.C., Yeh, C.C.: 'A unitary transformation method for angle-of-arrival estimation', *IEEE Trans. Signal Process.*, 1991, **39**, pp. 975–977
18 Linebarger, D.A., DeGroat, R.D., Dowling, E.M.: 'Efficient direction finding methods employing forward backward averaging', *IEEE Trans. Signal Process.*, 1994, **42**, pp. 2136–2145
19 Haardt, M.: 'Efficient one-two and multidimensional high-resolution array signal processing'. PhD dissertation, Technical University Munich, Munich, Germany, 1997
20 Stoica, P., Jansson, M.: 'On forward–backward MODE for array signal processing', *Digit. Signal Process.*, 1997, **7**, (4), pp. 239–252
21 Stoica, P., Nehorai, A.: 'MUSIC maximum likelihood and Cramer-Rao bound', *IEEE Trans. Acoust. Speech Signal Process.*, 1989, **37**, pp. 720–741